Int. J. Heat Mass Transfer. Vol. 33, No. 9, pp. 2029–2037, 1990
Printed in Great Britain

0017–9310/90 $3.00 + 0.00
© 1990 Pergamon Press plc

Turbulent fluid flow and heat transfer in concentric annuli with moving cores

T. SHIGECHI,† N. KAWAE† and Y. LEE‡

†Department of Mechanical Engineering, Nagasaki University, Nagasaki 852, Japan
‡Department of Mechanical Engineering, University of Ottawa, Ottawa, Canada K1N 6N5

(*Received* 6 *June* 1989 *and in final form* 17 *November* 1989)

Abstract—The momentum and heat transfer between a fully developed turbulent fluid flow and a moving core of fluid or solid body in concentric annular geometry is studied analytically based on a modified turbulence model. The heating condition is a uniform heat flux at the core tube only. The effects of various parameters such as the relative velocity, the radius ratio, etc. on friction factor and Nusselt number are investigated.

1. INTRODUCTION

PROBLEMS involving fluid flow and a moving core of fluid or solid body in an annular geometry are encountered in some practical situations. A train travelling at high speed in a long tunnel (such as the 54 km long Seikan tunnel in Japan, the proposed Channel Tunnel between England and France [1] or the proposed Northumberland Strait undersea tunnel linking Prince Edward Island and New Brunswick in eastern Canada), where a significant amount of thermal energy may be transferred to the tunnel environment. In certain manufacturing processes such as extrusion, hot rolling and drawing, a hot plate or cylindrical rod continuously exchanges heat with the surrounding environment. The inverted annular film boiling which takes place during the emergency core cooling of nuclear fuel channels [2] is another example which involves such fluid flow and heat transfer phenomena. For such cases, there seems to be no reliable prediction for momentum and heat transfer available in the literature.

In this paper, a new basic flow model, essential for the heat transfer analysis, is presented and the resulting momentum and heat transfer are discussed in terms of various parameters, such as the relative velocity, the radius ratio, fluid Reynolds number, etc.

2. ANALYSIS

In order to predict temperature distribution and heat transfer rates, it is necessary to predict velocity field and shear stress distribution in the gap between the stationary surface and the moving core. A simple modified mixing length model for flow turbulence is used for the analysis. The mathematical development of the analysis is straightforward but more intermediate details can be easily deduced from some standard reference books such as that by Kays and Crawford [3].

2.1. *Assumptions* (*see Fig. 1*)

(i) The annulus is concentric and both the wall surfaces are smooth. The heating condition is a uniform heat flux at the core tube only.

(ii) Velocity and temperature fields in the annulus are fully developed.

(iii) The axial pressure gradient is sufficiently large so that there exists a maximum velocity within the annulus.

(iv) The line of the maximum velocity coincides with the line of the zero shear stress.

(v) For the momentum eddy diffusivity, ε_M, the model by van Driest for the sublayer and that of Reichardt for the fully turbulent region are used.

(vi) The turbulent Prandtl number is either constant or a known function.

2.2. *Velocity and temperature distributions*

For the velocity and temperature distributions, use is made of the concept of eddy diffusivity, ε, and the turbulent Prandtl number, Pr_t. The basic equations governing the transport of momentum and heat can thus be written as

$$\frac{\tau_j}{\rho} = (\nu + \varepsilon_M)\frac{\hat{c}u_j}{\hat{c}y_j} \tag{1}$$

$$-\frac{q}{c\rho} = (\alpha + \varepsilon_H)\frac{\hat{c}T}{\hat{c}r}. \tag{2}$$

Equation (1) can be nondimensionalized as

$$\frac{\hat{c}u_j^+}{\hat{c}\zeta_j} = \delta_j^+\left[\frac{(\tau_j/\tau_R)_j}{1+(\varepsilon_M/\nu)_j}\right] \quad (0 \leqslant \zeta_j \leqslant 1) \tag{3}$$

where from a force balance, the shear stress distribution is

$$\left(\frac{\tau}{\tau_R}\right)_j = \frac{(1-\zeta_j)\{1 \pm [\Delta_j\zeta_j\,(2 \pm \Delta_j)]\}}{[1 \pm \Delta_j\zeta_j]}$$

NOMENCLATURE

A	van Driest's constant
c	specific heat
f	friction factor
h	heat transfer coefficient
k	thermal conductivity
K	von Karman's constant
Nu	Nusselt number
P	pressure
Pr	Prandtl number
Pr_t	turbulent Prandtl number
q	heat flux
r	radial coordinate, R_i+y_i or R_o-y_o
R	radius
R_j^+	$R_j(\tau_R/\rho)_j^{0.5}/\nu$
Re	Reynolds number
T	temperature
T_j^+	$(T_{R_i}-T_j)c\tau_{R_j}/[q_{R_i}(\tau_{R_j}/\rho)^{0.5}]$
u	velocity in the x-direction
u_j^+	$u_j/(\tau_R/\rho)_j^{0.5}$
u_τ	$(\tau_R/\rho)^{0.5}$
U^+	$U/(\tau_{R_i}/\rho)^{0.5}$
U^*	dimensionless relative velocity, U/u_b
y	coordinate
y_j^+	$y_j(\tau_R/\rho)_j^{0.5}$.

Greek symbols

α	radius ratio, R_i/R_o; thermal diffusivity
δ_j	$\lvert R_m-R_j\rvert$
δ_j^+	$\delta_j(\tau_R/\rho)_j^{0.5}/\nu$
Δ_j	δ_j^+/R_j^+
ε	eddy diffusivity
ζ_j	y_j^+/δ_j^+
ν	viscosity
ρ	density
τ	shear stress.

Subscripts

b	bulk
H	heat
i	inner
j	i or o
m	corresponding to the maximum velocity point
M	momentum
o	outer
R	radius
s	at sublayer boundary
t	turbulent.

Superscript

+	quantity nondimensionalized.

where +ve for $j=$ i, −ve for $j=$ o, and

$$\zeta_j = y_j^+/\delta_j^+, \quad \Delta_j = \delta_j^+/R_j^+.$$

The initial conditions for equation (3) are

$$u_i^+ = U^+ \text{ at } \zeta_i = 0 \text{ and } u_o^+ = 0 \text{ at } \zeta_o = 0.$$

Equation (2) can also be nondimensionalized as

$$\frac{\partial T_j^+}{\partial \zeta_j} = \pm Pr\cdot\delta_j^+\left[\frac{(q_j/q_{R_i})}{1+(Pr/Pr_t)(\varepsilon_M/\nu)_j}\right] \quad (0\leqslant\zeta_j\leqslant 1) \tag{4}$$

where +ve for $j=$ i and −ve for $j=$ o. Since the heating condition is a uniform heat flux at the core tube only, the heat flux distributions are obtained from an energy balance as

$$(q_i/q_{R_i}) = \frac{1-\alpha^2(1+\Delta_i\zeta_i)^2}{(1-\alpha^2)(1+\Delta_i\zeta_i)} \quad (0\leqslant\zeta_i\leqslant 1)$$

and

$$(q_o/q_{R_i}) = \frac{\alpha(2-\Delta_o\zeta_o)\Delta_o\zeta_o}{(1-\alpha^2)(1-\Delta_o\zeta_o)} \quad (0\leqslant\zeta_o\leqslant 1).$$

The initial conditions for equation (4) are

$$T_i^+ = 0 \text{ at } \zeta_i = 0 \text{ and } T_o^+ = T_{om}^+ \text{ at } \zeta_o = 1.$$

The dimensionless velocity and temperature distributions in the inner and outer regions of the maximum velocity (see Fig. 1) can now be obtained by solving these dimensionless differential equations, equations (3) and (4), respectively, once the eddy diffusivities and the matching conditions are established.

2.3. *Eddy diffusivity for momentum*, ε_M

For the eddy diffusivity for momentum, ε_M, the models originally due to van Driest [4] and Reichardt [5] were modified to suit the present flow channel geometry as:

for sublayers $(0\leqslant y_j^+\leqslant y_{js}^+)$

$$(\varepsilon_M/\nu)_j = K_j^2 y_j^{+2}[1-\exp(-y_j^+/A_j^+)]^2|\partial u_j^+/\partial y_j^+|; \tag{5}$$

for fully turbulent layers $(y_{js}^+\leqslant y_j^+\leqslant\delta_j^+)$

$$(\varepsilon_M/\nu)_j = [(K_j\delta_j^+)/6][1-(1-y_j^+/\delta_j^+)^2][1+2(1-y_j^+/\delta_j^+)^2]. \tag{6}$$

Equations (5) and (6) are further reduced as:

for $(0\leqslant\zeta_j\leqslant\zeta_{js})$

$$\left(\frac{\varepsilon_M}{\nu}\right)_j = \frac{1}{2}\left[-1+\left\{1+4(K_j\delta_j^+)^2\zeta_j^2\left[1-\exp\left(-\frac{\delta_j^+\zeta_j^+}{A_j^+}\right)\right]^2(\tau/\tau_R)_j\right\}^{0.5}\right] \tag{7}$$

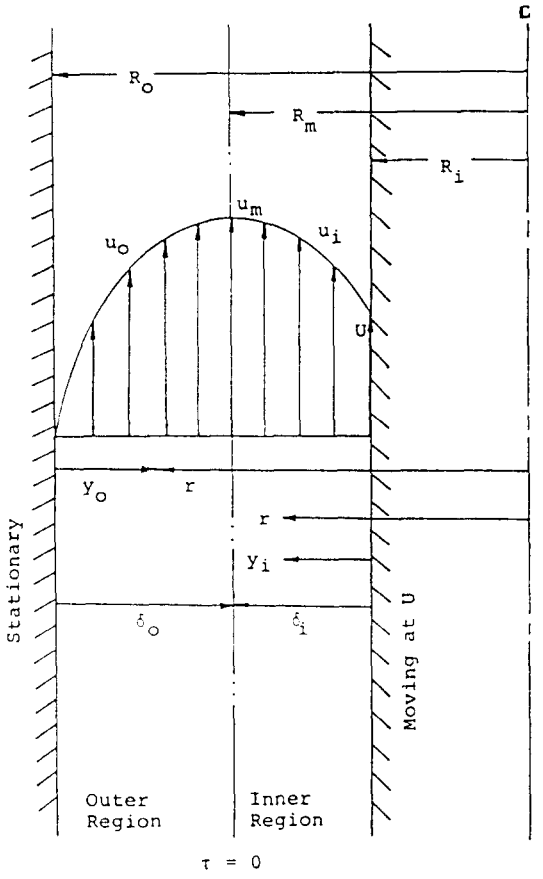

FIG. 1. Idealized model.

where

$$\zeta_{js} = y_{js}^{+}/\delta_j^{+};$$

for $(\zeta_{js} \leqslant \zeta_j \leqslant 1)$

$$(\varepsilon_M/\nu)_j = [(K_j\delta_j^{+})/6]\zeta_j(2-\zeta_j)(3-4\zeta_j+2\zeta_j^2). \quad (8)$$

2.4. *Reynolds number, friction factor and Nusselt number*

Now that the eddy diffusivities, $(\varepsilon_M/\nu)_j$, are known for the entire fluid regions, the velocity and temperature profiles can be derived. The Reynolds number, friction factor, heat transfer coefficient and Nusselt number are defined in the usual way as follows.

Reynolds number

$$Re = \frac{u_b \cdot 2(R_o - R_i)}{\nu} \quad (9)$$

where u_b is the average velocity defined by

$$u_b = \frac{1}{\pi(R_o^2 - R_i^2)}\left[\int_{R_i}^{R_m} u_i 2\pi r\,\mathrm{d}r + \int_{R_m}^{R_o} u_o 2\pi r\,\mathrm{d}r\right]. \quad (10)$$

Introducing the dimensionless parameter, u_b can be rewritten as

$$u_b = \left(\frac{\nu}{R_o}\right)\left[\frac{2\alpha}{1-\alpha^2}\right]\left[\delta_i^{+}\int_0^1 (1+\Delta_i\zeta_{si})u_i^{+}\,\mathrm{d}\zeta_{si} + \frac{1}{\alpha}\delta_o^{+}\int_0^1 (1-\Delta_o\zeta_{so})u_o^{+}\,\mathrm{d}\zeta_{so}\right]. \quad (11)$$

Therefore, in dimensionless parameters

$$Re = \left[\frac{4}{1+\alpha}\right]\left[\alpha\delta_i^{+}\int_0^1 (1+\Delta_i\zeta_{si})u_i^{+}\,\mathrm{d}\zeta_{si} + \delta_o^{+}\int_0^1 (1-\Delta_o\zeta_{so})u_o^{+}\,\mathrm{d}\zeta_{so}\right]. \quad (12)$$

Friction factor

$$f = \frac{(R_o - R_i)}{\rho u_b^2}\left(-\frac{\mathrm{d}P}{\mathrm{d}x}\right). \quad (13)$$

Equation (13), in conjunction with a force balance, can be given in a dimensionless form as

$$f = 8\left\{\frac{[1-(1/\alpha)]^2[1+(1/\alpha)(\tau_{R_i}/\tau_{R_i})]}{[1+(1/\alpha)]}\right\}\left(\frac{R_i^{+}}{Re}\right)^2. \quad (14)$$

Nusselt number

$$Nu = \frac{h \cdot 2(R_o - R_i)}{k} \quad (15)$$

where

$$h = q_{R_i}/(T_{R_i} - T_b).$$

The bulk temperature, T_b, is defined as

$$T_b = \int_{R_i}^{R_o} ruT\,\mathrm{d}r \Big/ \int_{R_i}^{R_o} ru\,\mathrm{d}r. \quad (16)$$

T_b can be expressed in dimensionless form as

$$T_b^{+} = \frac{(T_{R_i} - T_b)c\tau_{R_i}}{q_{R_i}(\tau_R/\rho)^{0.5}} = \left[\frac{4}{1+\alpha}\right]\left(\frac{1}{Re}\right)\left[\alpha\delta_i^{+}\int_0^1 (1+\Delta_i\zeta_{si})u_i^{+}T_i^{+}\,\mathrm{d}\zeta_{si} + \left(\frac{\tau_{R_i}}{\tau_{R_o}}\right)^{0.5}\delta_o^{+}\int_0^1 (1-\Delta_o\zeta_{so})u_o^{+}T_o^{+}\,\mathrm{d}\zeta_{so}\right]. \quad (17)$$

Therefore, the Nusselt number may be calculated from

$$Nu = 2\left[\frac{1-\alpha}{\alpha}\right]\frac{R_i^{+}\,Pr}{T_b^{+}}. \quad (18)$$

2.5. *Matching and other conditions*

The matching conditions for the analysis given above are given below.

(i) Shear stresses.

From a force balance

$$\frac{\tau_{R_i}}{\tau_{R_o}} = \left(\frac{1}{\alpha}\right)\left(\frac{R_m^2 - R_i^2}{R_o^2 - R_m^2}\right). \quad (19)$$

(ii) Relationship between K_i and K_o.

Although the mechanism of the flow outside of the radius of maximum velocity is very similar to that occurring in circular pipe flow, this is not true for the flow inside of the radius of the maximum velocity [6]. It is now well established that the standard universal velocity is not fully adequate for the inner velocity distribution of a concentric annulus [7, 8]. Therefore, while a fixed value of 0.4 for K_o is taken in the analysis, the value of K_i has to be calculated. From the continuity of the eddy diffusivity at the location of the maximum velocity ($r = R_m$ or $\zeta_i = \zeta_o = 1$), we may obtain the following relation from equation (8):

$$\frac{K_i}{K_o} = \frac{\delta_o^+}{\delta_i^+}. \tag{20}$$

(iii) Relationship between u_{im}^+ and u_{om}^+.

From the continuity of velocities at the location of the maximum velocity ($r = R_m$, or $\zeta_i = \zeta_o = 1$)

$$u_{om}^+ = \left(\frac{\tau_{R_i}}{\tau_{R_o}}\right)^{0.5} u_{im}^+. \tag{21}$$

(iv) Relationship between U^* and U^+.

$$U^* = \frac{2(1-\alpha)U^+ R_i^+}{\alpha\, Re}. \tag{22}$$

(v) Relationship between T_{im}^+ and T_{om}^+.

From the equality of temperature at the location of maximum velocity (i.e. $r = R_m$ or $\zeta_i = \zeta_o = 1$)

$$T_{om}^+ = (\tau_{R_o}/\tau_{R_i})^{0.5} T_{im}^+. \tag{23}$$

3. CALCULATION

To solve the equations given above, the following input and fixed parameters are provided for the calculation.

3.1. *Input parameters*

$\alpha = R_i/R_o$ —0.01, 0.2, 0.4, 0.6, 0.8 and 0.99
$R_i^+ = R_i u_{\tau i}/\nu$ —in terms of Re; 10^4–10^6
$U^+ = U/u_{\tau i}$ —in terms of U^*; 0, 0.2, 0.4, 0.6, 0.8 and 1.0
Pr —0.01, 0.1, 0.72, 1.0, 2, 5, 10 and 100
Pr_t —fixed at one for this paper.

3.2. *Fixed parameters*

$K_o = 0.4$ (von Karman's constant for outer region)
$A_o^+ = 26$ (van Driest damping parameter for outer region)
$A_i^+ = 26$ (van Driest damping parameter for inner region)
$y_{os}^+ = 26$ (sublayer thickness for outer region)
$y_{is}^+ = 26$ (sublayer thickness for inner region).

4. RESULTS AND DISCUSSION

The predicted velocity profiles in the annular ducts with the moving cores at various values of the relative velocity are presented in Fig. 2. The dimensionless velocity at the location of the maximum velocity does not coincide for a given condition. This is due to the different values of the wall shear stress at the walls, i.e. at $r = R_m$, or $\zeta_i = \zeta_o = 1$, the dimensionless velocity u_{om}^+ is related to u_{im}^+ through equation (21) and

$$\left.\frac{\partial u_o^+}{\partial \zeta_o}\right|_{\zeta_o = 1} = \left.\frac{\partial u_i^+}{\partial \zeta_i}\right|_{\zeta_i = 1} = 0. \tag{24}$$

As an example, the values of (τ_{R_i}/τ_{R_o}) at a Reynolds number of 10^5 are calculated as a function of U^* for $\alpha = 0.2$, 0.4, 0.6 and 0.8, and plotted in Fig. 3. The changes in the value of R_m as a function of α and U^* at a Reynolds number of 10^5 are also seen in Fig. 3.

In Fig. 4, the velocity profiles in both the inner

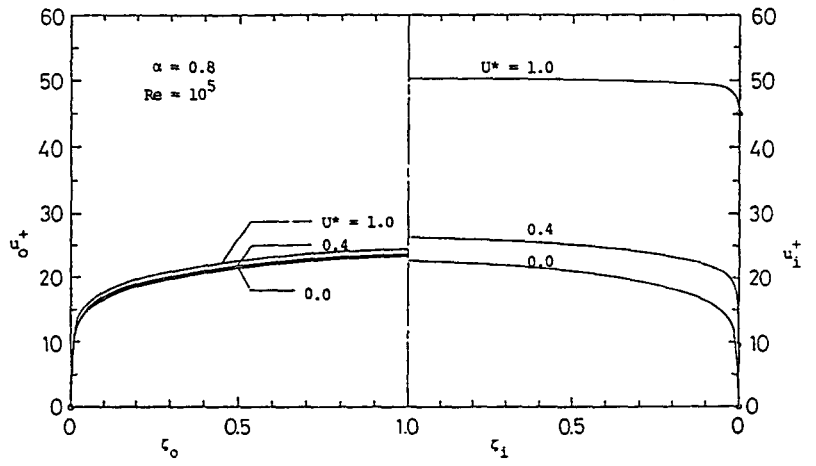

FIG. 2. Dimensionless velocity profiles.

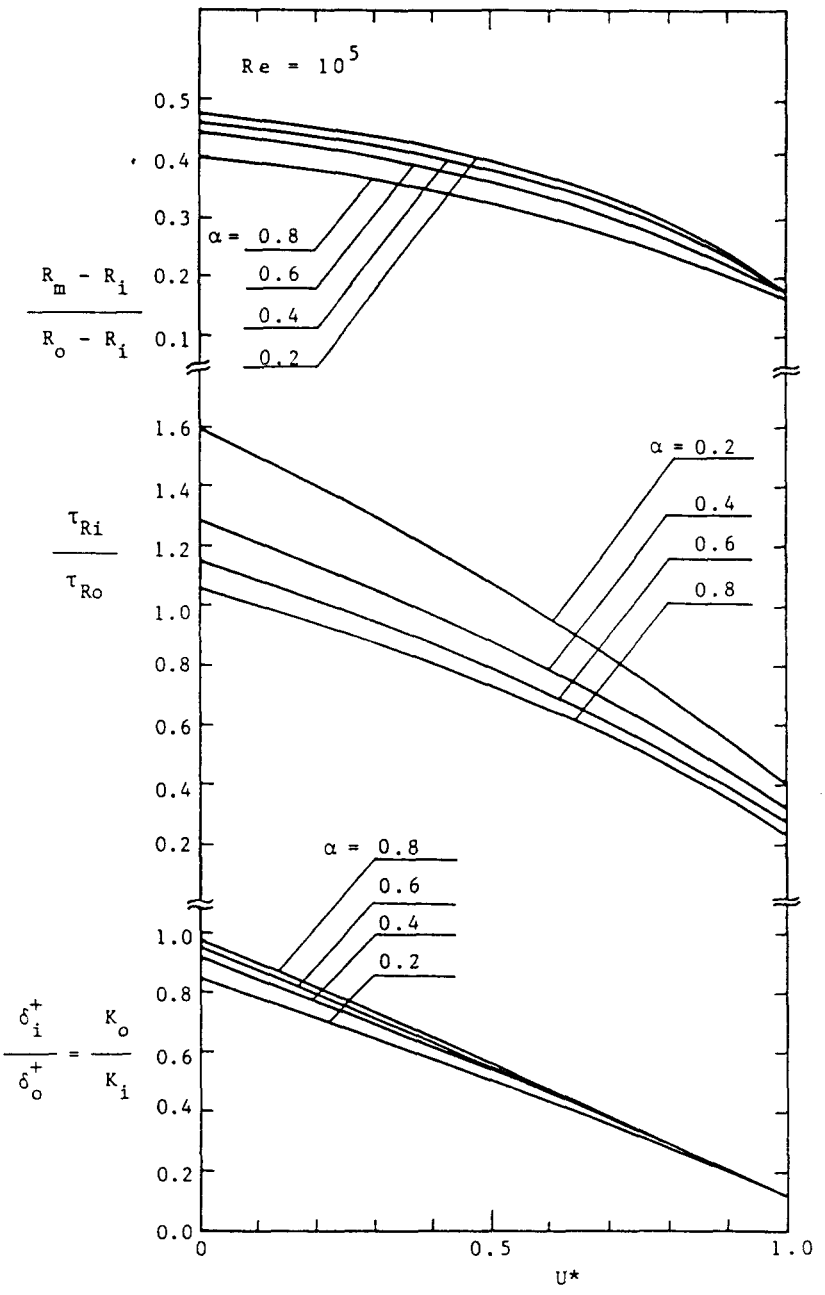

FIG. 3. Various relationships.

and outer regions are normalized by the maximum velocity. The strong effect of the relative velocity on the velocity profile in the inner region is now clearly seen in the figure.

Examples of the predicted friction factor are shown in Figs. 5 and 6. The values for the case of $U^* = 0$ (both walls stationary) are almost identical to the results of the previous analytical and experimental data [9]. This demonstrates the accuracy of the present analysis. The effect of the relative velocity is clearly shown in the figures.

The friction factor decreases with increasing values of the relative velocity, U^*, and the radius ratio, α, up to a certain critical value and then starts to increase again. However, the effect of the relative velocity diminishes with the decreasing value of the radius ratio and it was seen that at $\alpha = 0.01$, the effect is hardly seen at all. This is easily understandable because with decreasing value of α, the role of the shear stress of the inner surface on the overall pressure drop becomes less important.

Representative non-dimensional temperature pro-

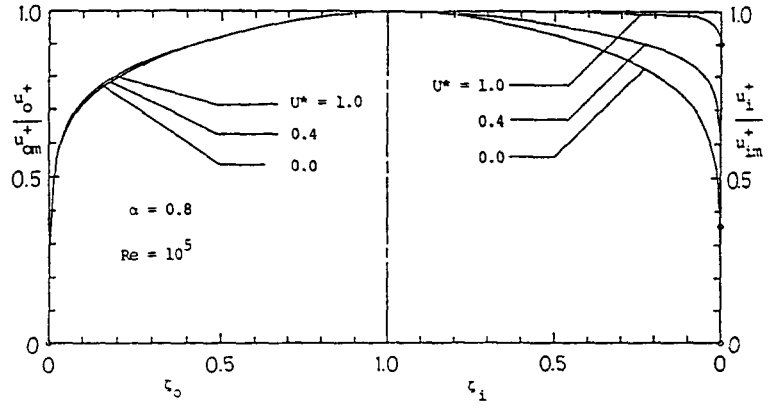

FIG. 4. Normalized velocity profiles.

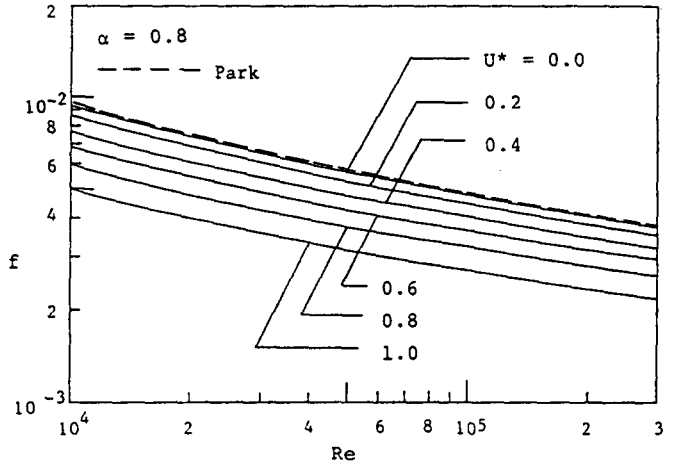

FIG. 5. Friction factor, $\alpha = 0.8$.

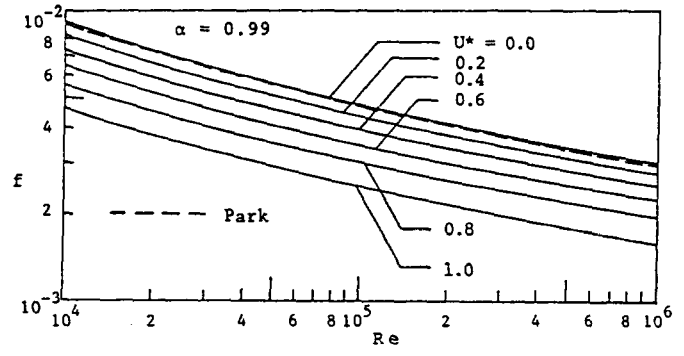

FIG. 6. Friction factor, $\alpha = 0.99$.

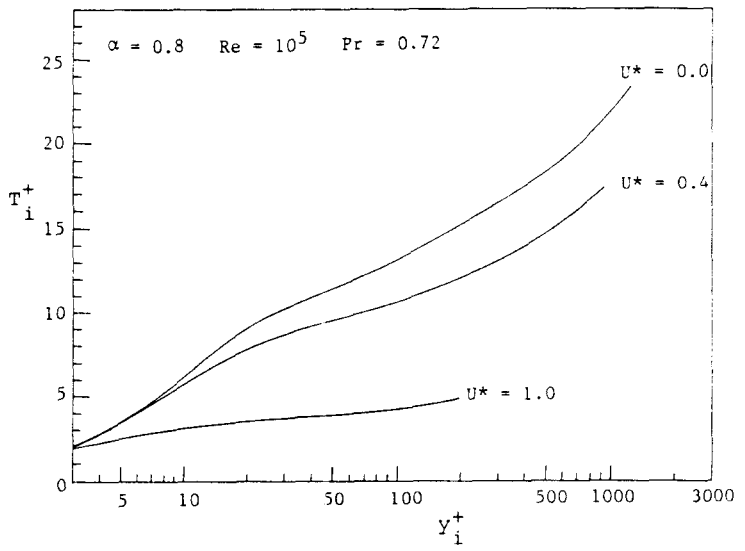

FIG. 7. Dimensionless temperature profiles; inner region.

files in the inner region of a concentric annulus with the moving core are shown in Fig. 7. The condition is for uniform heat flux at the core. The effect of the relative velocity can be clearly seen in the figure. The same temperature profiles of Fig. 7 are plotted in Fig. 8 in terms of normalized wall distance, ζ. As was seen in Fig. 2, the dimensionless temperature at the location of the maximum velocity does not coincide for a given condition and this is because different values of the wall shear stress at the walls were used in the dimensionless temperature parameters. That is, at $r = R_m$, or $\zeta_i = \zeta_o = 1$, the dimensionless velocity T^+_{om} is related to T^+_{im} through equation (23) and

$$\frac{\partial T_o^+}{\partial \zeta_o} = -\left(\frac{\delta_o^+}{\delta_i^+}\right)\frac{\partial T_i^+}{\partial \zeta_i}. \tag{25}$$

The values of $(\delta_i^+/\delta_o^+) = (K_o/K_i)$ at a Reynolds number of 10^5 are calculated as a function of U^* for $\alpha = 0.2$, 0.4, 0.6 and 0.8, and plotted in Fig. 3.

Predicted Nusselt numbers for two annuli having α of 0.2 and 0.8 are plotted against Reynolds number in Figs. 9 and 10, respectively, for various values of the relative velocity at a Prandtl number of 0.72. The effect of the relative velocity is seen to decrease with decreasing value of α as was the case of the effect on the friction factor shown in Figs. 5 and 6. However, the effect of the relative velocity on heat transfer is the opposite of that of friction factor; i.e. the heat transfer increases with increasing value of the relative velocity.

In Figs. 9 and 10, the analytical study of Kays and Leung [10] of concentric annuli with stationary cores (i.e. $U^* = 0$) when the inner core alone is heated is compared with that of the present analysis. Despite the different method of analysis employed, the agreement is very good for the range of parameters studied.

The effects of the radius ratio and Prandtl number on the fully developed Nusselt number at $U^* = 1$ are shown in Figs. 11 and 12, respectively, as examples. The effect of the radius ratio on heat transfer is similar

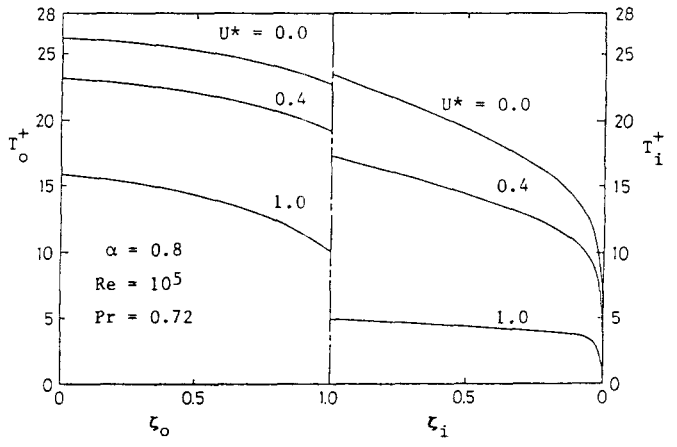

FIG. 8. Dimensionless temperature profiles; inner and outer regions.

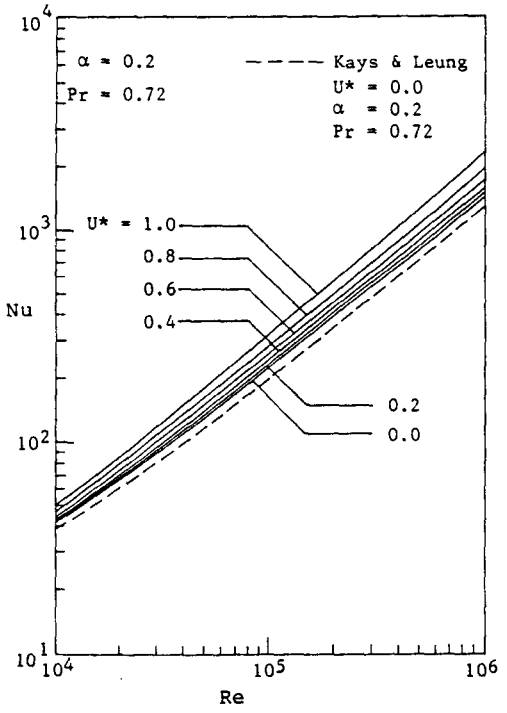

FIG. 9. Nusselt number; effect of relative velocity, $\alpha = 0.2$.

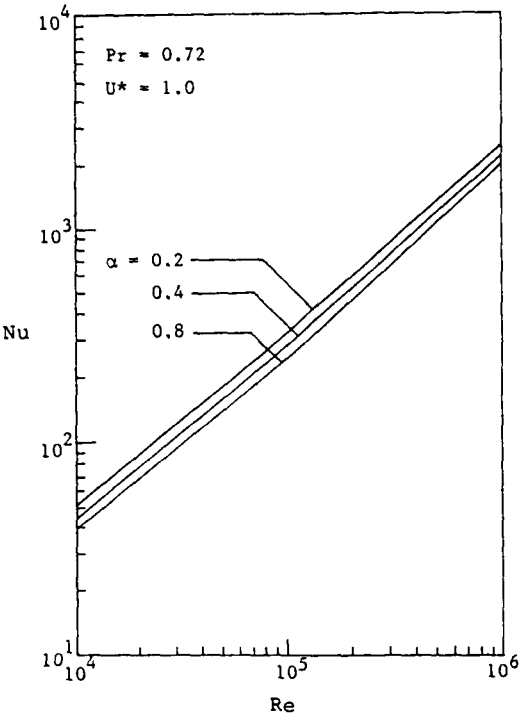

FIG. 11. Nusselt number; effect of radius ratio.

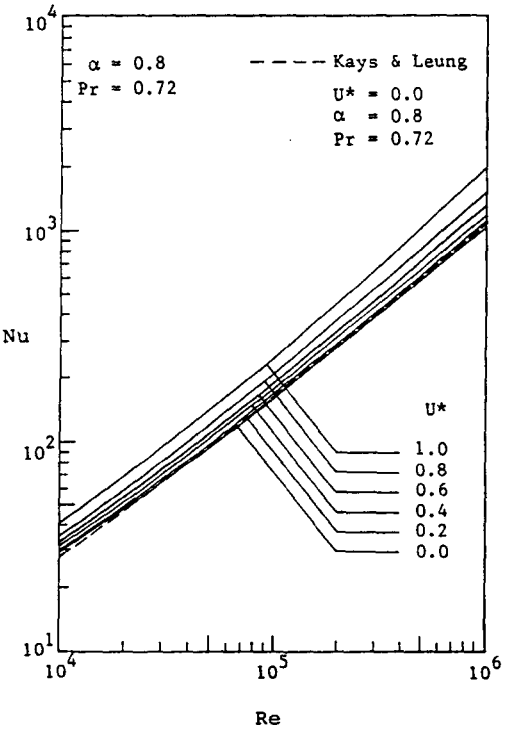

FIG. 10. Nusselt number; effect of relative velocity, $\alpha = 0.8$.

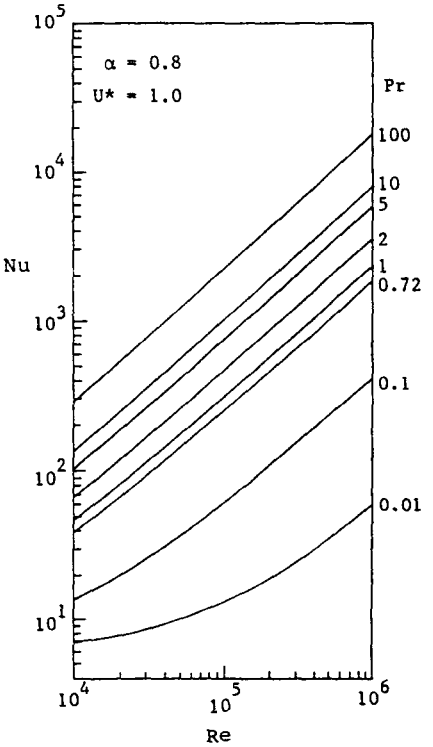

FIG. 12. Nusselt number; effect of Prandtl number.

to that for the case of $U^* = 0$, i.e. the lower the radius ratio, the higher the heat transfer rate but the effect is relatively minor. The effect of Prandtl number on Nusselt number is again similar to that for the case of an annulus with a stationary core tube, that is, the Nusselt number increases with increasing values of Prandtl number.

5. CONCLUDING REMARKS

The effects of various parameters such as relative velocity, radius ratio, etc. on the friction factor and Nusselt number for concentric annuli with moving cores have been analyzed.

The study showed that for equal conditions, increasing relative velocities were observed for the following changes:

- decrease in friction factor and
- increase in Nusselt number.

However, the effect of the relative velocity seems to diminish with decreasing value of the radius ratio.

REFERENCES

1. H. Barrow and C. W. Pope, A simple analysis of flow and heat transfer in railway tunnels, *Heat Fluid Flow* **8**, 119–123 (1987).
2. Y. Lee and K. H. Kim, Inverted annular flow boiling, *Int. J. Multiphase Flow* **13**, 345–355 (1987).
3. W. M. Kays and M. E. Crawford, *Convective Heat and Mass Transfer* (2nd Edn). McGraw-Hill, New York (1980).
4. E. R. van Driest, On turbulent flow near a wall, *J. Aero. Sci.* **23**, 485 (1956).
5. H. Reichardt, Vollstandige Darstellung der turbulenten Geschwindigkeitsverteilung in glatten Leitungen, *Z. Angew. Math. Mech.* **31**, 208–219 (1951).
6. H. Barrow, Y. Lee and A. Roberts, The similarity hypothesis applied to the turbulent flow in an annulus, *Int. J. Heat Mass Transfer* **8**, 1499–1505 (1965).
7. J. A. Brighton and J. B. Jones, Fully developed turbulent flow in annuli, *Trans. ASME, J. Basic Engng* **86**, 835–844 (1964).
8. V. K. Jonsson and A. Sparrow, Experiments on turbulent flow phenomena in eccentric annular ducts, *J. Fluid Mech.* **25**, 65–86 (1965).
9. S. D. Park, Developing turbulent flow and heat transfer in concentric annuli: an analytical and experimental study, Ph.D. Thesis, Department of Mechanical Engineering, University of Ottawa, Ottawa, Canada (1971).
10. W. M. Kays and E. Y. Leung, Heat transfer in annular passages—hydrodynamically developed turbulent flow with arbitrarily prescribed heat flux, *Int. J. Heat Mass Transfer* **6**, 537–557 (1963).

ECOULEMENT TURBULENT ET TRANSFERT THERMIQUE DANS DES ESPACES ANNULAIRES AVEC COEUR MOBILE

Résumé—Le transfert de quantité de mouvement et de chaleur entre un fluide en écoulement turbulent établi et un coeur mobile de fluide ou de solide, dans une géométrie annulaire concentrique, est étudié analytiquement à partir d'un modèle modifié de turbulence. La condition de chauffage est celle d'un flux thermique uniforme sur le tube central. On étudie les effets des paramètres tels que la vitesse relative, le rapport des rayons, etc. sur le coefficient de frottement et le nombre de Nusselt.

TURBULENTE STRÖMUNG UND WÄRMEÜBERGANG IN EINEM KONZENTRISCHEN RINGSPALT MIT BEWEGTEM KERN

Zusammenfassung—Die Impuls- und Wärme-Übertragung zwischen einer vollständig ausgebildeten, turbulenten Fluidströmung und einem bewegten Kern (ebenfalls fluid oder fest) wird für eine Anordnung als konzentrischer Ringspalt analytisch untersucht. Dabei wird ein modifiziertes Turbulenzmodell angewandt. Als Randbedingung am Kern wird aufgeprägte Wärmestromdichte angenommen. Der Einfluß von Relativgeschwindigkeit, Radienverhältnis, usw. auf den Reibungsbeiwert und die Nusselt-Zahl wird untersucht.

ТУРБУЛЕНТНОЕ ТЕЧЕНИЕ ЖИДКОСТИ И ТЕПЛОПЕРЕНОС В КОНЦЕНТРИЧЕСКИХ КОЛЬЦЕВЫХ КАНАЛАХ С ДВИЖУЩИМСЯ ЯДРОМ

Аннотация—На основе модифицированной модели турбулентности аналитически исследуется перенос импульса и тепла между полностью развитым турбулентным течением жидкости и движущимся ядром жидкости или твердого тела в концентрических кольцевых каналах. Нагрев происходит в условиях постоянного теплового потока у центральной трубы. Исследуется влияние на коэффициент трения и число Нуссельта таких параметров, как относительная скорость, отношение скоростей и т. д.